Bioorganic Chemistry 108 (2021) 104614

Contents lists available at ScienceDirect

Bioorganic Chemistry

journal homepage: www.elsevier.com/locate/bioorg

Short communication

Discovery and SAR studies of 3-amino-4-(phenylsulfonyl)tetrahydrothiophene 1,1-dioxides as non-electrophilic antioxidant response element (ARE) activators

Jeyun Jo [a,†], Lara Ibrahim [b,†], Jonathan Iaconelli [b], Jinsook Kwak [a], Manoj Kumar [c], Yunjin Jung [a], Luke L. Lairson [b], Arnab K. Chatterjee [c], Peter G. Schultz [b,c], Michael J. Bollong [b,*], Hwayoung Yun [a,b,*]

[a] College of Pharmacy, Pusan National University, Busan 46241, Republic of Korea
[b] Department of Chemistry, The Scripps Research Institute, 10550, North Torrey Pines, La Jolla, CA 92037, United States
[c] California Institute for Biomedical Research, 11119 North Torrey Pines Road, Suite 100, La Jolla, CA 92037, United States

ARTICLE INFO

Keywords:
ARE activator
NRF2
PGK1 inhibitor
Structure-activity relationship
Reactive metabolites

ABSTRACT

The transcription factor NRF2 controls resistance to oxidative insult and is thus a key therapeutic target for treating a number of disease states associated with oxidative stress and aging. We previously reported CBR-470-1, a bis-sulfone which activates NRF2 by increasing the levels of methylglyoxal, a metabolite that covalently modifies NRF2 repressor KEAP1. Here, we report the design, synthesis, and structure activity relationship of a series of bis-sulfones derived from this unexplored chemical template. We identify analogs with sub-micromolar potencies, **7f** and **7g**, as well as establish that efficacious NRF2 activation can be achieved by non-toxic analogs **7c**, **7e**, and **9**, a key limitation with CBR-470-1. Further efforts to identify non-covalent NRF2 activators of this kind will likely provide new insight into revealing the role of central metabolism in cellular signaling.

1. Introduction

Persistent oxidative stress and exposure to electrophilic xenobiotics promote aging and age-related diseases such as cancer, chronic inflammation, cardiovascular disease, and neurodegeneration [1,2]. Consequently, the mammalian cell has evolved an inducible transcriptional program orchestrated by the transcription factor nuclear factor erythroid 2-related factor 2 (NRF2) to protect against oxidative insult [3]. In unstressed conditions, NRF2 is continually sent for proteasomal degradation by its cytoplasmic repressor and Cullin 3 adaptor protein, Kelch-like ECH-associated protein 1 (KEAP1) [4]. In response to oxidative injury or electrophilic challenge, cysteine 'sensor' residues in KEAP1 are oxidized or alkylated, a modification which promotes accumulation of NRF2 in the nucleus [4]. Licensed activation of NRF2 promotes upregulation of cytoprotective gene products containing conserved antioxidant response element (ARE) sites within their genomic loci [5].

A wide variety of small molecules capable of promoting ARE-regulated gene expression have been identified to date [6], including phenolic and flavonoid antioxidants [7], isothiocyanates [8], Michael acceptors [9], and organosulfur compounds [10]. As such, the majority of these molecules are electrophiles or are transformed in cells to form electrophiles, which promote ARE activation by covalent modification of KEAP1 [6]. Although electrophilic compounds such as dimethyl fumarate [11], bardoxolone methyl [12], and sulforaphane [8], have demonstrated clinical benefit or are FDA approved medications [13,14], electrophilic small molecules are typically not considered useful drug candidates because they broadly react with cellular nucleophiles causing cytotoxicity. Indeed, late stage clinical candidate bardoxolone methyl interacts with hundreds of cellular targets and displays cytotoxicity [15,16], despite impressive clinical efficacy in chronic kidney disease trials. These observations have prompted the development of non-covalent binders of the Kelch domain of KEAP1, molecules which inhibit KEAP1-mediated degradation of NRF2 [17]. While molecules like KI696 [18,19] and other KEAP1-NRF2 interaction inhibitors have shown protective activity in preclinical animal models, the comparative

* Corresponding authors.
E-mail addresses: mbollong@scripps.edu (M.J. Bollong), hyun@pusan.ac.kr (H. Yun).
† These authors contributed equally to this work.

https://doi.org/10.1016/j.bioorg.2020.104614
Received 11 September 2020; Received in revised form 13 November 2020; Accepted 28 December 2020
Available online 5 January 2021

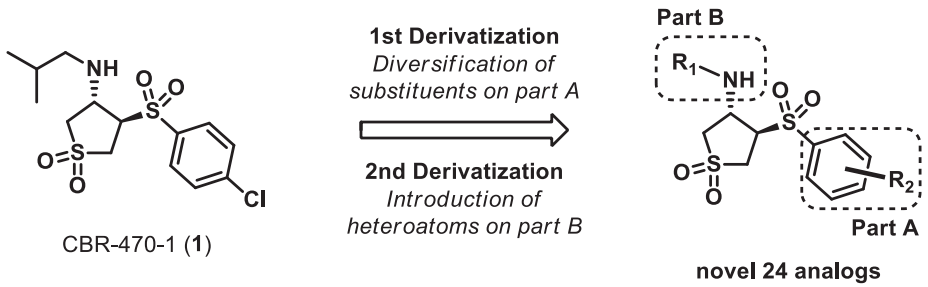

Fig. 1. Optimization strategy used in this work to identify novel 3-amino-4-(phenylsulfonyl)tetrahydrothiophene 1,1-dioxide derivatives.

efficacy of these series relative to covalent NRF2 activators has not been evaluated and the clinical potential of this compound class has not yet been realized.

As a central sensor and integrator of cellular redox status, KEAP1 relays metabolic information to the transcriptional activation of NRF2 through modification of KEAP1′s sensor cysteines. Several endogenous electrophilic metabolites have been demonstrated as covalent modifiers of KEAP1 by *S*-alkylation, driving NRF2-driven cellular adaptations in response to increased metabolic pathway flux. Key examples include fumarate [20,21] and itaconate [22,23], mitochondrial metabolites derived from the citric acid cycle that promote NRF2 activation in various physiological settings. Given this, we envisioned an alternative approach in which chemical libraries might be broadly interrogated for non-electrophilic small molecule activators of ARE transcription. In principle, such an approach might identify compounds that favorably modify metabolism to augment levels of KEAP1-reactive metabolites. Recently, we reported the discovery of CBR-470-1 (**1**, Fig. 1), a molecule derived from an unexplored 3-amino-4-(phenylsulfonyl) tetrahydrothiophene 1,1-dioxide skeleton, which activates NRF2 by inhibiting the glycolytic enzyme phosphoglycerate kinase 1 (PGK1) [24]. Pharmacological PGK1 inhibition promotes buildup of the triose phosphate degradation product methylglyoxal (MGO), a dicarbonyl we found intermolecularly inactivates KEAP1 by crosslinking proximal cysteine and arginine residues through a novel methylthioimidazole-based

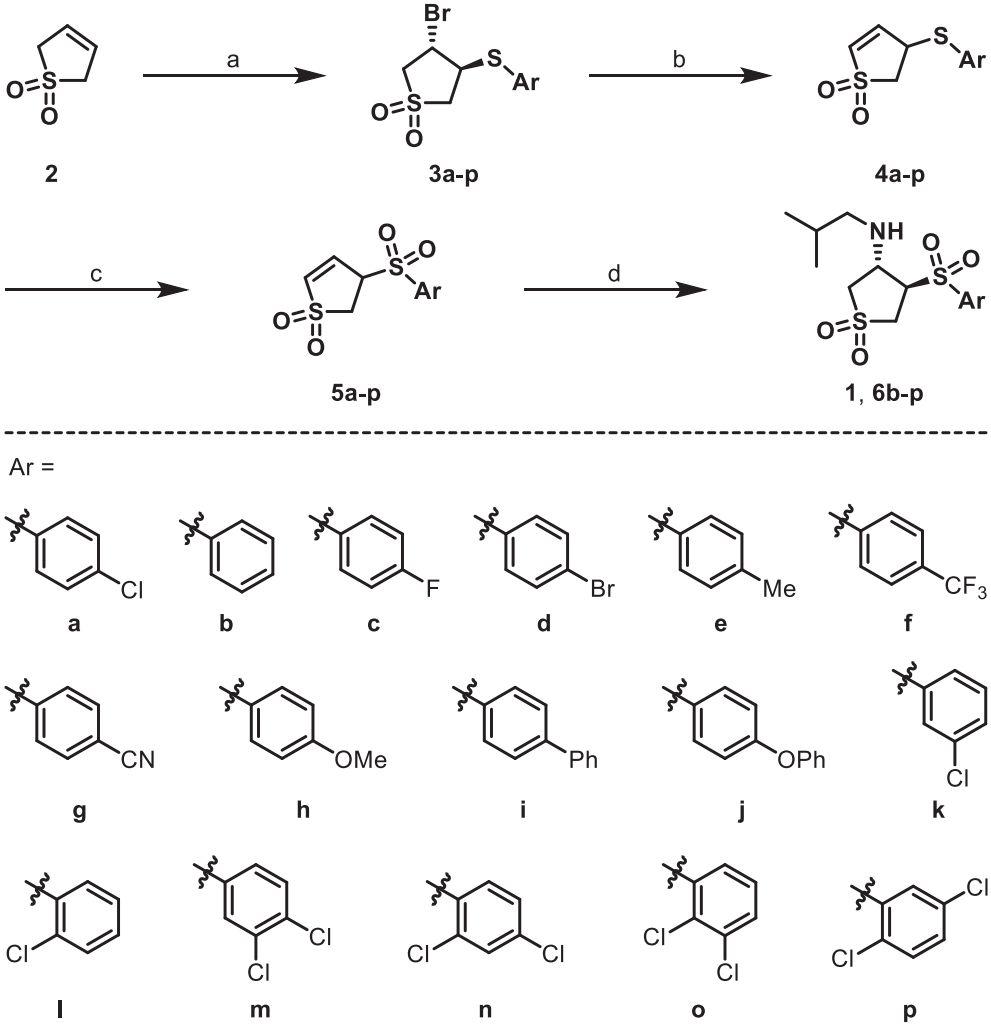

Scheme 1. Synthesis of analogs **1** and **6b-p**. Reagents and conditions: (a) Ar-SH, NBS, CH_2Cl_2, rt, 20–61%; (b) pyridine, CH_2Cl_2, 70 °C, 33–82%; (c) *m*CPBA, CH_2Cl_2, rt; (d) *i*-butylamine, CH_3CN, rt, 14–56% for 2 steps.

Table 1
ARE-LUC inductive activities of compounds **1** and **6b**–**6p**.

Comp.	ARE-LUC fold induction at 20 μM[a]	Comp.	ARE-LUC fold induction at 20 μM[a]
1	6.7	**6i**	7.9
6b	6.1	**6j**	12.7
6c	12.0	**6k**	7.1
6d	17.1	**6l**	4.3
6e	10.1	**6m**	20.0
6f	0.8	**6n**	0.0
6g	1.7	**6o**	2.1
6h	8.5	**6p**	0.6

[a] Values are the mean of three experiments.

modification, termed MICA [24].

As the molecular architecture of this chemical scaffold is largely unexplored and there are no other reported cell permeable inhibitors of PGK1, we engaged in the structural optimization of **1**. Herein, we describe the design, synthesis, and biological evaluation of this novel series of non-electrophilic ARE activators and a brief structure–activity relationship (SAR).

2. Result and discussion

The efficient and concise synthesis of derivatives of the phenylsulfone moiety (Part A) was carried out in four steps as depicted in Scheme 1. Bromosulfenylation of commercially available 3-sulfolene (**2**) and various thiophenols in the presence of *N*-bromosuccinimide afforded the desired β-bromosulfides **3a**–**p** [25]. Exposure of **3a**–**p** to pyridine in refluxing CH_2Cl_2 readily provided the dehydrobrominated thiophenes **4a**–**p** in good yield. Finally, sequential *m*-chloroperoxybenzoic acid (*m*CPBA) oxidations of **4a**–**p** and conjugate additions of the resulting bis-sulfones **5a**–**p** with isobutylamine furnished the desired β-aminosulfones **1** and **6b**–**p** in a one-pot process.

With this set of compounds, we investigated the effects of phenyl substitution using a NRF2-dependent ARE-LUC reporter assay in IMR32 cells. Eight of these analogs (**6c**–**6e**, **6h**-**6k**, and **6m**) displayed a greater ARE-activating response than compound **1** at 20 μM (Table 1). Removal of the chloro substituent on the benzene ring, as in compound **6b**, negatively affected ARE-LUC induction, while chloro substitution at the *meta*-position (**6k**) led to a slight increase in the ARE-LUC activation. In contrast, moving the substituent to the *ortho*-position (**6l**) resulted in a

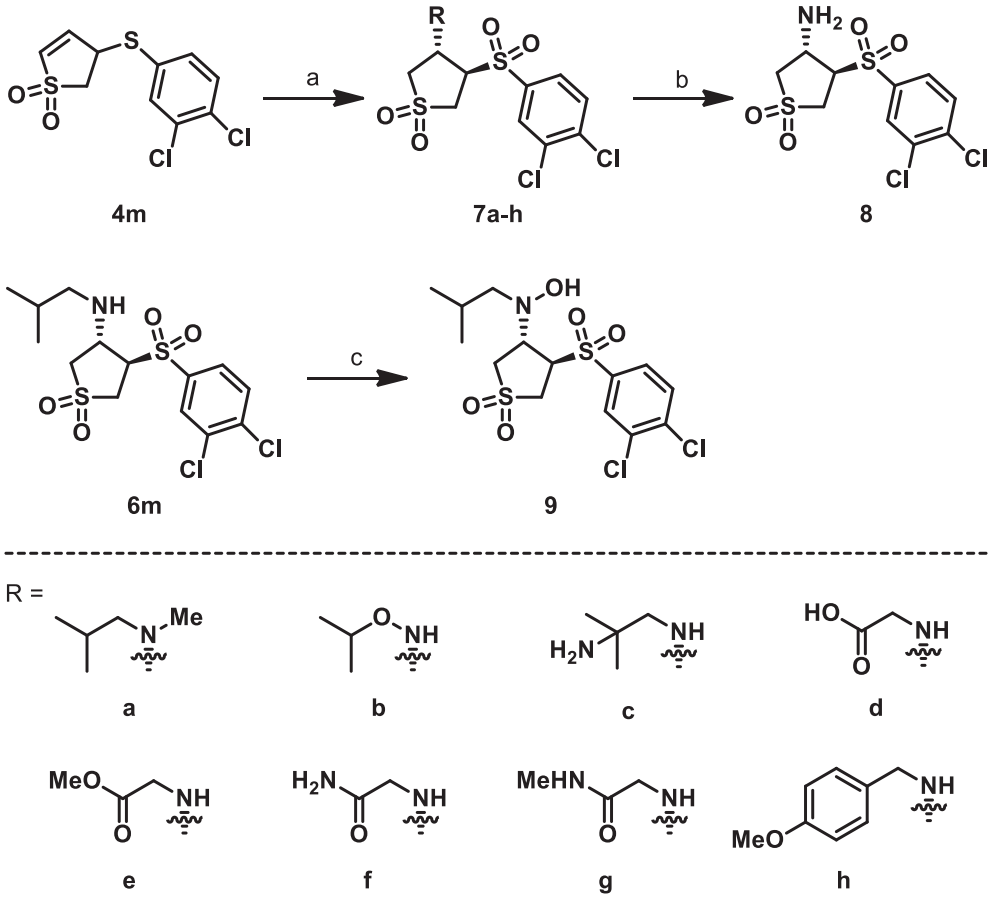

Scheme 2. Synthesis of analogs **7a**-**g**, **8** and **9**. Reagents and conditions: (a) *m*CPBA, CH_2Cl_2, rt; then various amines (except for d), *i*-Pr_2NEt, CH_3CN, rt, 17–41% for 2 steps; (b) $Ce(NH_4)_2(NO_3)_6$, CH_3CN/H_2O, rt, 54% from **7h** (c) *m*CPBA, $CHCl_3$, rt, 81%.

Table 2
ARE-LUC inductive activities and cytotoxicity of compounds **6m**, **7a**-**7g**, **8h**, and **9**.

Comp.	ARE-LUC EC_{50} [μM][a]	ARE-LUC E_{max} [FI][b]	IMR32 cytotoxicity IC_{50} [μM][c]
1	1.0	31.9	5.4
6m	3.6	20.0	5.6
7a	1.0	52.6	7.0
7b	>20	6.9	>20
7c	1.0	55.0	>20
7d	1.0	56.0	9.9
7e	1.1	45.6	>20
7f	0.8	36.7	12.7
7g	0.7	30.5	9.0
8	2.4	74.0	0.3
9	1.8	99.7	>20

[a] EC_{50} values are the mean of three experiments and correspond to the concentration resulting in half-maximal induction for each compound.
[b] FI, fold induction relative to a DMSO neutral stimulation control.
[c] IC_{50} values are the mean of three experiments and correspond to the concentration of each compound which results in 50% cytotoxicity.

small decrease in the activity. Among derivatives monosubstituted at position 4 of this ring (**6c**–**6j**), those possessing an electron-donating group (**6e** and **6h**–**6j**) displayed more efficacious ARE-inducing activities compared to those bearing an electron-withdrawing group (**6f** and **6g**), except for halide analogs **6c** and **6d**. The most active compound was 3,4-dichloro substituted analog **6m**, which displayed about three-fold increase in ARE-LUC-inducing activity relative to **1**. Low ARE activation was observed with other disubstituted analogs **6n**–**6p** at the tested concentration, which is possibly derived from enhanced cytotoxicity at this concentration.

We next turned our attention to modification of the *i*-butylamino group of **6m**. Our established synthetic procedure allowed for the design and synthesis of analogs modified on part B of the scaffold as in **7a**–**g**, **8**, and **9** (Scheme 2). Sulfide oxidation of **4m**, followed by conjugate additions of the resulting bis-sulfone **5m** with the indicated amines produced the final β-aminosulfones **7a**–**g** (except for the glycine derivative **7d** [26]) and the advanced intermediate **7h** in a one-pot process. Oxidative cleavage of the PMB protected bis-sulfone **7h** provided the *N*-dealkylated analog **8** in moderate yield. The hydroxylamine derivative **9** was obtained by *m*CPBA oxidation of **6m** in good yield.

From our initial investigation of SAR and preliminary metabolite identification profiling (Figs. S1 and S2) we were encouraged to probe the influence of the aminoalkyl substitutions on part B of the bis-sulfone scaffold. We evaluated the maximal fold-induction (E_{max}) and the EC_{50} of analogs in concentration-dependent ARE-LUC reporter assays and assessed their cytotoxic activity (Table 2). Generally, analogs with modified substituents on the amine showed enhanced potency to **6 m**, except for the *O*-isopropylhydroxylamino compound **7b**. *N*-methylation (**7a**) or introduction of an amino group on the tertiary carbon (**7c**) improved both potency and transcriptional efficacy. A similar increase in ARE-LUC activity was also observed for analogs in which the *i*-butylamino group was replaced with glycine (**7d**) or glycine methyl ester (**7e**). It is noteworthy that **7c** and **7e** had no cytotoxic potential toward IMR32 cells, suggesting that PGK1 activity and likely thus glycolytic flux can be modulated without obligate cytotoxicity. The most potent compounds evaluated were amide substituted **7f** and **7g**, which displayed submicromolar potency with similar E_{max} values to **1**. *N*-dealkylated analog **8**, a major expected metabolite of **6m**, was found to be most toxic although it exhibited an approximate 3.5-fold enhancement of the efficacy relative to the parent compound. In contrast, putative *N*-hydroxyl metabolite **9** had the highest E_{max} value (99.7-FI) with no evidence of toxicity below 20 μM. These results suggest that the ARE-inducing activity and cytotoxicity of this scaffold can be manipulated by single modifications to the aminoxy moiety (Part B) of the bis-sulfone scaffold. These results also underscore the effectiveness of using metabolite identification experiments in medicinal chemistry campaigns, given the divergent activities on cytotoxicity and ARE-LUC activity of identified metabolites in this work (i.e., **8** vs. **9**).

3. Conclusion

In summary, we report the design, synthesis, and biological evaluation of a series of bis-sulfone ARE activator molecules, based on CBR-470–1 (**1**). Our SAR results suggest that the phenylsulfone region (Part A) of the scaffold can be substituted with a number of groups to improve the magnitude of ARE induction relative to **1**. We also demonstrate that Part B, the *i*-butylamino moiety of **1**, can be substituted to improve potency of the series below 1 μM, as demonstrated by **7f** and **7g**. Lastly, we show that **7c**, **7e**, and presumptive metabolite **9** efficaciously activate NRF2 transcriptional activity without cytotoxicity below 20 μM. Importantly, this result suggests that PGK1 can be engaged in cells without obligate cytotoxicity, a current limitation with the use of **1** for studies involving protective NRF2 activation. Together these results provide a roadmap for the future modification of this scaffold to identify non-toxic molecules with enhanced potencies and the requisite physicochemical features for *in vivo* studies, a result we will report in future work.

4. Experimental

4.1. Chemistry

Unless noted otherwise, all starting materials and reagents were obtained from commercial suppliers and were used without further purification. Reaction flasks were dried at 100 °C. Air- and moisture-sensitive reactions were performed under an argon atmosphere. All solvents used for routine isolation of products and chromatography were reagent-grade. Flash column chromatography was performed using silica gel 60 (230–400 mesh, Merck) with the indicated solvents. Thin-layer chromatography was performed using 0.25 mm silica gel plates (Merck). ^{1}H and $^{13}C\{^{1}H\}$ NMR spectra were recorded on Bruker AMX-400 (400 MHz), AVANCE NEO 500, and Unity-Inova 500 (500 MHz) instruments and calibrated using residual solvent peaks as internal reference. Chemical shifts were expressed in parts per million (ppm, δ) downfield from tetramethylsilane and calibrated to the deuterated solvent reference peak. ^{1}H NMR data were reported in the order of chemical shift, multiplicity (s, singlet; d, doublet; t, triplet; q, quartet; m, multiplet and/or multiple resonance), number of protons, and coupling constant quoted in hertz (Hz). Preparative high-pressure liquid chromatography (prep-HPLC) was operated on Agilent Technologies 1200 Infinity Series. High-resolution mass spectrometry (HR-MS) data were obtained with an Agilent LC/MSD TOF mass spectrometer by electrospray ionization-time of flight (ESI-TOF) reflectron experiments.

4.1.1. 3-Bromo-4-((3,4-dichlorophenyl)thio)tetrahydrothiophene 1,1-dioxide (3m) [24]

To a stirred solution of *N*-bromosuccinimide (4.26 g, 25.4 mmol) in CH_2Cl_2 (60.0 mL) was added dropwise a solution of 3,4-dichlorobenzenethiol (3.23 mL, 25.4 mmol). After stirred for 30 min, to the reaction mixture was added dropwise a solution of 3-sulfolene **2** (3.00 g, 25.4 mmol). After stirring for 2 h, the reaction mixture was quenched with H_2O. The aqueous layer was extracted with CH_2Cl_2 and the combined organic layers were dried over $MgSO_4$ and concentrated *in vacuo*. The residue was purified by flash column chromatography on silica gel (EtOAc : *n*-hexane = 1 : 5) to afford 4.75 g (50%) of **3m** as white solid: ^{1}H NMR ($CDCl_3$, 500 MHz) δ 7.60 (d, 1H, J = 2.1 Hz), 7.47 (d, 1H, J = 8.3 Hz), 7.34 (dd, 1H, J = 8.3, 2.1 Hz), 4.34 (q, 1H, J = 7.1 Hz), 4.04 (q, 1H, J = 7.4 Hz), 3.93 (dd, 1H, J = 14.1, 7.1 Hz), 3.73 (dd, 1H, J = 13.7, 7.4 Hz), 3.51 (dd, 1H, J = 14.1, 6.9 Hz), 3.14 (dd, 1H, J = 13.9, 7.4 Hz); $^{13}C\{^{1}H\}$ NMR ($CDCl_3$, 100 MHz) δ 135.3, 134.2, 133.8, 133.0, 131.6, 130.4, 59.4, 55.9, 51.9, 43.4; LR-MS (ESI+) *m/z* 375 $[M + H]^+$; HR-MS (ESI+)

calculated for $C_{10}H_{10}BrCl_2O_2S_2$ $[M + H]^+$ 374.8677; found 374.8679.

4.1.2. 3-((3,4-Dichlorophenyl)thio)-2,3-dihydrothiophene 1,1-dioxide (4m) [24]

To a stirred solution of **3m** (487 mg, 1.29 mmol) in CH_2Cl_2 (10.0 mL) was added pyridine (0.260 mL, 3.23 mmol). After stirring for 1 h at 70 ℃, the reaction mixture was cooled to rt and quenched with saturated aq. NH_4Cl. The aqueous layer was extracted with CH_2Cl_2 and the combined organic layers were dried over $MgSO_4$ and concentrated *in vacuo*. The residue was purified by flash column chromatography on silica gel (EtOAc : *n*-hexane = 1 : 2) to afford 310 mg (81%) of **4m** as white solid: ^{1}H NMR ($CDCl_3$, 400 MHz) δ 7.55 (d, 1H, J = 2.1 Hz), 7.44 (d, 1H, J = 8.3 Hz), 7.28 (dd, 1H, J = 8.4, 2.2 Hz), 6.71 (m, 1H), 6.69 (m, 1H), 4.47 (m, 1H), 3.66 (dd, 1H, J = 14.1, 8.2 Hz), 3.21 (dd, 1H, J = 14.1, 4.5 Hz); ^{13}C{^{1}H} NMR ($CDCl_3$, 100 MHz) δ 138.8, 135.2, 134.1, 133.7, 133.6, 132.9, 131.4, 130.7, 54.4, 45.0; LR-MS (ESI+) *m/z* 295 $[M + H]^+$; HR-MS (ESI+) calculated for $C_{10}H_9Cl_2O_2S_2$ $[M + H]^+$ 294.9416; found 294.9416.

4.1.3. 3-((3,4-Dichlorophenyl)sulfonyl)-4-(isobutylamino) tetrahydrothiophene 1,1-dioxide (6m) [24]

To a stirred solution of **4m** (310 mg, 1.05 mmol) in CH_2Cl_2 (10.0 mL) was added *m*CPBA (648 mg, 2.63 mmol, 70 ~ 75%). After stirring for 1 h, the reaction mixture was filtered and quenched with saturated aq. $NaHCO_3$. The aqueous layer was extracted with CH_2Cl_2 and the combined organic layers were dried over $MgSO_4$ and concentrated *in vacuo*. The crude mixture was used for next step without further purification. To a stirred solution of the sulfone in CH_3CN (10.0 mL) was added *i*-butylamine (0.104 mL, 1.05 mmol). After stirring for 1 h, the reaction mixture was concentrated *in vacuo*. The residue was purified by preparative HPLC and lyophilized to afford 215 mg (51%) of **6m** as white solid: ^{1}H NMR (DMSO-d_6, 400 MHz) δ 8.21 (d, 1H, J = 2.0 Hz), 7.96 (d, 1H, J = 8.4 Hz), 7.90 (dd, 1H, J = 8.4, 2.1 Hz), 4.38 (q, 1H, J = 8.5 Hz), 3.66 (m, 3H), 3.42 (dd, 1H, J = 14.1, 9.0 Hz), 3.12 (dd, 1H, J = 12.2, 6.0 Hz), 2.17 (m, 1H), 2.03 (m, 1H), 1.87 (q, 1H, J = 7.7 Hz), 1.31 (m, 1H), 0.67 (d, 3H, J = 3.9 Hz), 0.65 (d, 3H, J = 3.9 Hz); ^{13}C{^{1}H} NMR (DMSO-d_6, 100 MHz) δ 138.5, 137.6, 132.4, 131.6, 130.6, 128.7, 63.5, 55.4, 55.1, 54.4, 49.4, 28.0, 20.3; LR-MS (ESI+) *m/z* 400 $[M + H]^+$; HR-MS (ESI+) calculated for $C_{14}H_{20}Cl_2NO_4S_2$ $[M + H]^+$ 400.0205; found 400.0204.

4.1.4. 3-((3,4-Dichlorophenyl)sulfonyl)-4-(hydroxy(isobutyl)amino) tetrahydrothiophene 1,1-dioxide (9)

To a stirred solution of **6m** (50.0 mg, 125 μmol) in $CHCl_3$ (1.0 mL) was added *m*CPBA (30.8 mg, 125 μmol, 70 ~ 75%). After stirring for 3 h, the reaction mixture was filtered and the filtrate was quenched with saturated aq. $NaHCO_3$. The aqueous layer was extracted with CH_2Cl_2 and the combined organic layers were dried over $MgSO_4$ and concentrated *in vacuo*. The residue was purified by prep-HPLC and lyophilized to afford 42.1 mg (81%) of **9** as white solid: ^{1}H NMR (DMSO-d_6, 400 MHz) δ 8.14 (d, 1H, J = 2.0 Hz), 7.94 (d, 1H, J = 8.4 Hz), 7.87 (dd, 1H, J = 8.4, 2.0 Hz), 4.42 (q, 1H, J = 8.7 Hz), 4.02 (q, 1H, J = 8.1 Hz), 3.74 (dd, 1H, J = 14.4, 9.4 Hz), 3.46 (m, 3H), 2.24 (dd, 1H, J = 12.3, 4.8 Hz), 2.02 (dd, 1H, J = 12.2, 9.3 Hz), 1.57 (m, 1H), 0.71 (d, 3H, J = 6.8 Hz), 0.53 (d, 3H, J = 6.5 Hz); ^{13}C{^{1}H} NMR (DMSO-d_6, 125 MHz) δ 138.3, 137.7, 132.5, 131.8, 130.6, 128.8, 65.2, 63.3, 61.7, 49.3, 47.8, 25.4, 20.5, 19.8; LR-MS (ESI+) *m/z* 416 $[M + H]^+$; HR-MS (ESI+) calculated for $C_{14}H_{20}Cl_2NO_5S_2$ $[M + H]^+$ 416.0154; found 416.0151.

4.2. ARE-LUC assay

For miniaturized reporter assays, 5000 IMR32 cells (ATCC, routinely tested for mycoplasma contamination) were plated per well in white 384-well plates (Corning) in 40 μL of growth medium: DMEM (Corning), 10% fetal bovine serum (FBS, Gibco) and 1% Penicillin-Streptomycin (Pen-Strep, Gibco). 24 h after plating, 100 ng of reporter plasmid, pTI-ARE-LUC, was transferred to each well in 10 μL of Opti-MEM medium (Gibco), diluted from a master stock composed such that 1 μg of reporter plasmid was complexed with 4 μL of FugeneHD (Promega). The next day, serial DMSO dilutions of compounds in a 384-well source plate were transferred to the above assay plate using a PerkinElmer FX instrument outfitted with a 100 nL pintool head (VP Scientific). After 24-hour incubation, ARE-LUC luminance values were recorded on an Envision plate reader (PerkinElmer) after the addition of 30 μL of BrightGlo (diluted 1:3 in water) with shaking.

4.3. Cellular viability assay

For miniaturized viability assays, 5000 IMR32 cells were plated per well in white 384-well plates in 50 μL of growth medium. The next day, cells were treated with compounds via pintool-based transfer, as above. After a 24-hour incubation, cellular viability measurements were recorded after the addition of 30 μL of CellTiterGlo solution (Promega, diluted 1:6 in water) on an Envision plate reader.

Declaration of Competing Interest

The authors declare that they have no known competing financial interests or personal relationships that could have appeared to influence the work reported in this paper.

Acknowledgments

This work was supported by the Skaggs Institute for Chemical Biology at Scripps Research and the Bio & Medical Technology Development Program of the National Research Foundation (NRF) funded by the Korean government (MSIT) (NRF-2017M3A9G7072568). We thank Kristen Williams for technical support with manuscript preparation. We are especially grateful for the assistance of the Compound Management Group (CMG) at Calibr, namely Alonzo Davila and Emily Roddy.

Appendix A. Supplementary data

Supplementary data to this article can be found online at https://doi.org/10.1016/j.bioorg.2020.104614.

References

[1] I. Liguori, G. Russo, F. Curcio, G. Bulli, L. Aran, D. Della-Morte, G. Gargiulo, G. Testa, F. Cacciatore, D. Bonaduce, P. Abete, Oxidative stress, aging, and diseases, Clin. Interv. Aging 13 (2018) 757–772.
[2] H. Sies, C. Berndt, D.P. Jones, Oxidative Stress, Annu. Rev. Biochem. 86 (2017) 715–748.
[3] Q. Ma, Role of nrf2 in oxidative stress and toxicity, Annu Rev Pharmacol Toxicol 53 (2013) 401–426.
[4] P. Canning, F.J. Sorrell, A.N. Bullock, Structural basis of Keap1 interactions with Nrf2, Free Radic. Biol. Med. 88 (Pt B) (2015) 101–107.
[5] C. Tonelli, I.I.C. Chio, D.A. Tuveson, Transcriptional Regulation by Nrf2, Antioxid. Redox Signal 29 (17) (2018) 1727–1745.
[6] W. Hur, N.S. Gray, Small molecule modulators of antioxidant response pathway, Curr. Opin. Chem. Biol. 15 (1) (2011) 162–173.
[7] K.C. Wu, P.R. McDonald, J. Liu, C.D. Klaassen, Screening of natural compounds as activators of the keap1-nrf2 pathway, Planta Med. 80 (1) (2014) 97–104.
[8] Y. Zhang, P. Talalay, C.G. Cho, G.H. Posner, A major inducer of anticarcinogenic protective enzymes from broccoli: isolation and elucidation of structure, Proc. Natl. Acad. Sci. USA 89 (6) (1992) 2399–2403.
[9] V. Kumar, S. Kumar, M. Hassan, H. Wu, R.K. Thimmulappa, A. Kumar, S.K. Sharma, V.S. Parmar, S. Biswal, S.V. Malhotra, Novel chalcone derivatives as potent Nrf2 activators in mice and human lung epithelial cells, J. Med. Chem. 54 (12) (2011) 4147–4159.
[10] L.W. Wattenberg, E. Bueding, Inhibitory effects of 5-(2-pyrazinyl)-4-methyl-1,2-dithiol-3-thione (Oltipraz) on carcinogenesis induced by benzo[a]pyrene, diethylnitrosamine and uracil mustard, Carcinogenesis 7 (8) (1986) 1379–1381.
[11] M. Wakkee, H.B. Thio, Drug evaluation: BG-12, an immunomodulatory dimethylfumarate, Curr. Opin. Investig. Drugs 8 (11) (2007) 955–962.
[12] M.S. Yates, M. Tauchi, F. Katsuoka, K.C. Flanders, K.T. Liby, T. Honda, G. W. Gribble, D.A. Johnson, J.A. Johnson, N.C. Burton, T.R. Guilarte, M. Yamamoto, M.B. Sporn, T.W. Kensler, Pharmacodynamic characterization of chemopreventive

triterpenoids as exceptionally potent inducers of Nrf2-regulated genes, Mol. Cancer Ther. 6 (1) (2007) 154–162.
[13] S. Celentano, G. Capolongo, R.M. Pollastro, Bardoxolone: a new potential therapeutic agent in the treatment of autosomal dominant polycystic kidney disease? G Ital. Nefrol. 36 (5) (2019).
[14] H. Kanda, K. Yamawaki, Bardoxolone methyl: drug development for diabetic kidney disease, Clin. Exp. Nephrol. (2020).
[15] M.M. Yore, A.N. Kettenbach, M.B. Sporn, S.A. Gerber, K.T. Liby, Proteomic analysis shows synthetic oleanane triterpenoid binds to mTOR, PLoS One 6 (7) (2011), e22862.
[16] X.Y. Wang, X.H. Zhang, L. Peng, Z. Liu, Y.X. Yang, Z.X. He, H.W. Dang, S.F. Zhou, Bardoxolone methyl (CDDO-Me or RTA402) induces cell cycle arrest, apoptosis and autophagy via PI3K/Akt/mTOR and p38 MAPK/Erk1/2 signaling pathways in K562 cells, Am. J. Transl. Res. 9 (10) (2017) 4652–4672.
[17] J.S. Pallesen, K.T. Tran, A. Bach, Non-covalent Small-Molecule Kelch-like ECH-Associated Protein 1-Nuclear Factor Erythroid 2-Related Factor 2 (Keap1-Nrf2) Inhibitors and Their Potential for Targeting Central Nervous System Diseases, J. Med. Chem. 61 (18) (2018) 8088–8103.
[18] T.G. Davies, W.E. Wixted, J.E. Coyle, C. Griffiths-Jones, K. Hearn, R. McMenamin, D. Norton, S.J. Rich, C. Richardson, G. Saxty, H.M. Willems, A.J. Woolford, J. E. Cottom, J.P. Kou, J.G. Yonchuk, H.G. Feldser, Y. Sanchez, J.P. Foley, B. J. Bolognese, G. Logan, P.L. Podolin, H. Yan, J.F. Callahan, T.D. Heightman, J. K. Kerns, Monoacidic Inhibitors of the Kelch-like ECH-Associated Protein 1: Nuclear Factor Erythroid 2-Related Factor 2 (KEAP1:NRF2) Protein-Protein Interaction with High Cell Potency Identified by Fragment-Based Discovery, J. Med. Chem. 59 (8) (2016) 3991–4006.
[19] T.D. Heightman, J.F. Callahan, E. Chiarparin, J.E. Coyle, C. Griffiths-Jones, A. S. Lakdawala, R. McMenamin, P.N. Mortenson, D. Norton, T.M. Peakman, S. J. Rich, C. Richardson, W.L. Rumsey, Y. Sanchez, G. Saxty, H.M.G. Willems, L. Wolfe, A.J. Woolford, Z. Wu, H. Yan, J.K. Kerns, T.G. Davies, Structure-Activity and Structure-Conformation Relationships of Aryl Propionic Acid Inhibitors of the Kelch-like ECH-Associated Protein 1/Nuclear Factor Erythroid 2-Related Factor 2 (KEAP1/NRF2) Protein-Protein Interaction, J. Med. Chem. 62 (9) (2019) 4683–4702.
[20] J. Adam, E. Hatipoglu, L. O'Flaherty, N. Ternette, N. Sahgal, H. Lockstone, D. Baban, E. Nye, G.W. Stamp, K. Wolhuter, M. Stevens, R. Fischer, P. Carmeliet, P. H. Maxwell, C.W. Pugh, N. Frizzell, T. Soga, B.M. Kessler, M. El-Bahrawy, P. J. Ratcliffe, P.J. Pollard, Renal cyst formation in Fh1-deficient mice is independent of the Hif/Phd pathway: roles for fumarate in KEAP1 succination and Nrf2 signaling, Cancer Cell 20 (4) (2011) 524–537.
[21] A. Ooi, J.C. Wong, D. Petillo, D. Roossien, V. Perrier-Trudova, D. Whitten, B. W. Min, M.H. Tan, Z. Zhang, X.J. Yang, M. Zhou, B. Gardie, V. Molinie, S. Richard, P.H. Tan, B.T. Teh, K.A. Furge, An antioxidant response phenotype shared between hereditary and sporadic type 2 papillary renal cell carcinoma, Cancer Cell 20 (4) (2011) 511–523.
[22] M. Bambouskova, L. Gorvel, V. Lampropoulou, A. Sergushichev, E. Loginicheva, K. Johnson, D. Korenfeld, M.E. Mathyer, H. Kim, L.H. Huang, D. Duncan, H. Bregman, A. Keskin, A. Santeford, R.S. Apte, R. Sehgal, B. Johnson, G. K. Amarasinghe, M.P. Soares, T. Satoh, S. Akira, T. Hai, C. de Guzman Strong, K. Auclair, T.P. Roddy, S.A. Biller, M. Jovanovic, E. Klechevsky, K.M. Stewart, G. J. Randolph, M.N. Artyomov, Electrophilic properties of itaconate and derivatives regulate the IkappaBzeta-ATF3 inflammatory axis, Nature 556 (7702) (2018) 501–504.
[23] E.L. Mills, D.G. Ryan, H.A. Prag, D. Dikovskaya, D. Menon, Z. Zaslona, M. P. Jedrychowski, A.S.H. Costa, M. Higgins, E. Hams, J. Szpyt, M.C. Runtsch, M. S. King, J.F. McGouran, R. Fischer, B.M. Kessler, A.F. McGettrick, M.M. Hughes, R. G. Carroll, L.M. Booty, E.V. Knatko, P.J. Meakin, M.L.J. Ashford, L.K. Modis, G. Brunori, D.C. Sevin, P.G. Fallon, S.T. Caldwell, E.R.S. Kunji, E.T. Chouchani, C. Frezza, A.T. Dinkova-Kostova, R.C. Hartley, M.P. Murphy, L.A. O'Neill, Itaconate is an anti-inflammatory metabolite that activates Nrf2 via alkylation of KEAP1, Nature 556 (7699) (2018) 113–117.
[24] M.J. Bollong, G. Lee, J.S. Coukos, H. Yun, C. Zambaldo, J.W. Chang, E.N. Chin, I. Ahmad, A.K. Chatterjee, L.L. Lairson, P.G. Schultz, R.E. Moellering, A metabolite-derived protein modification integrates glycolysis with KEAP1-NRF2 signalling, Nature 562 (7728) (2018) 600–604.
[25] C.C.T. Ko, Preparation and Reactions of Benzofurano-, Indolo-, and Benzothieno-3-sulfolenes, J. Org. Chem. 63 (1998) 4645–4653.
[26] R. Moellering, J. Coukos, G. Lee, J.W. Chang, G. Mutlu, Compositions And Methods For Activating NRF2-Dependent Gene Expression. 2019. WO 2020/081446 Al.